# Design and Test of a Low-Damage Garlic Seeding Device Based on Rigid-Flexible Coupling

Siyuan Wang , YuBai Meng , Yongjian Wang * , Hua Li , Xiaodong Zhang

Posted Date: 9 September 2025

doi: 10.20944/preprints202509.0664.v1

Keywords: low-damage; garlic; seeding device; rigid-flexible coupling

 doi:10.20944/preprints202509.0664.v1



*Article*

# Design and Test of a Low-Damage Garlic Seeding Device Based on Rigid-Flexible Coupling

**Siyuan Wang [1], YuBai Meng [2], Yongjian Wang [1,*], Hua Li [1] and Xiaodong Zhang [1]**

[1] College of Engineering, Nanjing Agricultural University, Nanjing 210031, China

[2] College of Mechanical and Power Engineering, Nanjing Tech University, Nanjing 211816, China

* Correspondence: Yongjian Wang, yjwang@njau.edu.cn;

**Abstract**

In the context of the conventional mechanized garlic seeding process, the issue of damage to garlic seeds is a pervasive challenge that is challenging to circumvent. This paper proposes a solution to this problem by designing and testing a garlic seeding device that incorporates a rigid-flexible coupling mechanism. The purpose of this innovation is to mitigate the damage to garlic seeds during the sowing process. Firstly, the seeding pocket is constructed from a flexible metal sheet, which functions as its structural foundation. A slider along the fixed track enables the retraction and release of the pocket, thereby facilitating the process of collecting and dropping garlic seeds. Secondly, the effects of pocket radius, rotational speed of seed discharge disc and thickness of metal sheet on the stress of garlic seeds were investigated through finite element method. Finally, the experimental bench was set up to analyze the effects of pocket radius, rotational speed of seed discharge disc and thickness of metal sheet on the damage rate, single-seed rate and leakage rate. Results demonstrated that under optimal parameters—a pocket radius of 12 mm, a seed discharge disc rotational speed of 0.21 rad/s, and a metal sheet thickness of 0.15 mm—the proposed mechanism achieved a single-seed rate of 78.4%, a leakage rate of 11.4%, and a maximum stress on garlic seeds of only 0.535 MPa. Significantly, this stress level is well below the damage threshold of garlic seeds, resulting in a remarkably zero damage that outperforms conventional rigid seeding devices. This demonstrates the mechanism's remarkable capacity to safeguard the integrity of the seeds, even though the effect of the seeding process is comparatively low and shows considerable scope for enhancement in future iterations.

**Keywords:** low-damage; garlic; seeding device; rigid-flexible coupling

## 1. Introduction

Garlic is a globally significant cash crop, with annual production exceeding 28 million tons [1,2]. It is valued for its culinary and medicinal properties [3–5]. However, mechanized seeding operations are characterized by persistent issues pertaining to seed damage rates that frequently exceed 12% [6]. This phenomenon can be attributed to the inherent irregular geometry, fragile epidermis and variable clove sizes that are intrinsic to garlic bulbs. The occurrence of mechanical injury [7] during the process of seeding, which may manifest as epidermal bruising, internal fractures, or germ damage, has been demonstrated to result in a reduction of germination rates by 15–30% and a compromise to yield potential by 6%, thereby constituting a critical bottleneck in the context of sustainable garlic production. Conversely, the enhancement of seeding quality emerges as the most direct and effective technical measure to achieve an increase in the yield per unit area [6–9]. It is evident that the design of the garlic seeding device, which is based on a rigid-flexible coupling, is of great practical significance in reducing damage to garlic seeds during the seeding process.

The primary challenges associated with precision seeding technology pertain to the prevention and reduction of damage to seeds. A substantial corpus of research has been conducted by numerous scholars about issues pertaining to seed damage in seeding device. In the field of mechanical seeding

 doi:10.20944/preprints202509.0664.v1



device [8], scholars have conducted systematic research from three perspectives: mechanical optimization, material modification, and biomimetic design. Li et al. [9] optimized the angle of the seed wheel (from 15° to 25°) using EDEM simulation, thereby reducing the collision acceleration of corn seeds by 62.5%, lowering the seed damage rate from 8.7% to 2.1%, and increasing the single-seed rate to 96.5%. In the study by Landahl et al. [10], the metal clamping components were substituted with polyurethane elastic finger clamps, resulted in a 48% reduction in peak contact stress (from 1.8 MPa to 0.94 MPa) and a decrease in soybean seed coat damage rate from 12.3% to 3.8%. Wang et al. [11] developed a speed-adaptive release mechanism based on seed fall trajectory prediction, which increased the rate of seed impact energy absorption by 73%. Furthermore, the rate of rice hull cracking was reduced from 9.2% to 1.7%. Those studies have explored low-damage seeding for specific crops and achieved significant damage reduction effects. However, garlic seeds differ markedly from these crops in terms of morphology, physical properties, and other aspects, and the low-damage seeding technology still requires in-depth exploration. Nevertheless, the research results mentioned above provide highly valuable references for the development of low-damage seeding for garlic seeds.

For the garlic seeding, existing research has predominantly focused on improving seeding quality, specifically with the core objectives of increasing the single-seed rate and reducing the leakage rate. Ding et al [12] designed a finger clip plate garlic seeding device that uses a circular truncated cone seed-collecting scoop and splint driven by fine adjustment spring to achieve low-damage seed extraction. Under optimal experimental conditions (finger clip angle of 63°, spoon diameter of 24 mm, and rotation speed of 34 r/min), bench testing showed a single-seed rate of 91.86% and a leakage rate of 2.71%. Hou's team addressed the technical bottlenecks in single-seed of garlic, successively developing the chain spoon-type [13], wheel spoon-type [14], double charging chamber-type [15], and dragon claw-type seeding devices [16]. However, mechanical hard contact is likely to be injurious to the seed. This is particularly evident in the case of large seeds, such as those of garlic, where the structure of the seed extraction mechanism in the seed box is subject to poor seed's flow, resulting in the occurrence of friction damage to the garlic seeds. The clamping mechanism has been observed to result in injury to the garlic seed, attributable to excessive clamping force during the seed-carrying process. However, research on seed damage during garlic sowing is relatively scarce. Zilpilwar et al [17] developed a cup-feed metering mechanism, achieving a minimal mechanical damage rate of 5.7% in field tests.

Pneumatic seeders employ airflow to adsorb and transport the seeds, thereby offering the inherent advantage of reduced damage in comparison to mechanical seeders [18]. Relevant studies have primarily focused on airflow field regulation and changes in adsorption posture [18–20], with the core objectives of improving the single-seed rate and reducing the leakage rate. However, these studies have not directly addressed the stress state of seeds during the seeding process, and thus cannot quantitatively measure the damage caused to seeds. Meanwhile, the configuration of pneumatic seed extraction structures is complex, requiring auxiliary air pumps and related accessory devices, which leads to increased costs. Furthermore, the force exerted on seeds is positively correlated with both pressure magnitude and aperture size; improper design may still result in damage to seeds.

This paper proposed a conceptualization of a garlic precision seeding device equipped with a variable diameter track and pocket capture mechanism. The cooperation between the pocket, which contains a flexible metal sheet that functions as the skeleton, and the rigid slider along the fixed track is adopted to realize the retraction and release of the pocket. The analysis of the seeding process by pocket was conducted utilizing the finite element method. An experimental test was constructed, and the optimal working parameters combination was determined through the implementation of a second-order orthogonal experiment.

 doi:10.20944/preprints202509.0664.v1



## 2. Design of the Seeding Device

### *2.1. Structure of the Seeding Device*

The configuration of the rigid-flexible coupled garlic seeding device is illustrated in Figure 1. The apparatus consists of a rotating disc, a fixed disc, six sliding bars, six sliders, six seeding pockets, a main shaft, a seed box, a disturbance plate, a camshaft, a cam, and a seed chamber housing. The fixed disc is mounted on the outer housing and features specific tracks that control the reciprocating motion of the sliders. The rotating disc is connected to the main shaft via a hexagonal groove structure at its center. The sliding bars are secured to the rotating disc with screws, and the metal sheets with pockets are fixed to the end of the sliding bars. The disturbance plate is located on the seed chamber housing, at the bottom of the seed box. The cam, positioned below and in contact with the disturbance plate, is connected to the camshaft via a key. The camshaft is connected to the main shaft via a chainwheel. The structural design is analogous to the finger-clip design [12,21], yet it is distinguished by the integration of flexible metal sheets.

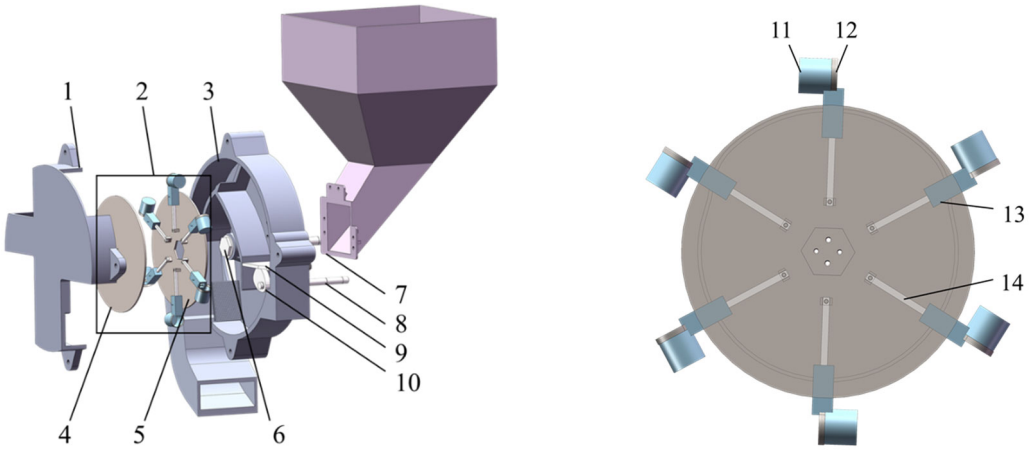


(a) Exploded view of the overall structure (b) Structure of the seed metering disc

**Figure 1.** Structure of the seeding device (1. Front cover 2. Seed tray 3. Seed chamber 4. Fixed disc 5. Rotating disc 6. Main shaft 7. Seed box 8. Camshaft 9. Disturbance plate 10. Cam 11. Seeding pocket 12. Metal sheet 13. Slider 14 Sliding bar).

### *2.2. Principle of the Seeding Device*

The seeding device is divided into three distinct areas, namely the seed collection area, the seed carrying area, and the seed sowing area, based on its operational state (see Figure 2).

During the operation, seeds fall from the seed box onto the disturbance plate in the seed collection area. The camshaft is responsible for driving the cam to rotate, thereby inducing vibrations to the disturbance plate. The disturbance caused by the disturbance plate results in a more dispersed garlic seed population in the seed collection area, thereby increasing its flowability. The lower end of the seed population is subjected to the impact force from the disturbance plate and the gravitational resistance of the seed population, facilitating the entry of the garlic seeds below into the seeding pockets. Each seeding pocket remains open in this area, rotates together with the rotating disc, and during this process, it may pick up 1–2 garlic seeds.

Within the designated seed carrying area, the seeding pockets undergo a process of tightening, resulting in the secure enclosure of the garlic seeds. This ensures that the seeds are transported in a stable manner to the designated seed sowing area. The metal sheet's flexibility ensures that the garlic seed is not damaged during the tightening process, while enhancing both adaptability to garlic seeds and gripping stability.

Upon entering the seed sowing area, the sliders retract, causing the pockets to open. Subsequently, the seeds descend under the force of gravity, thereby completing the seeding process.

 doi:10.20944/preprints202509.0664.v1



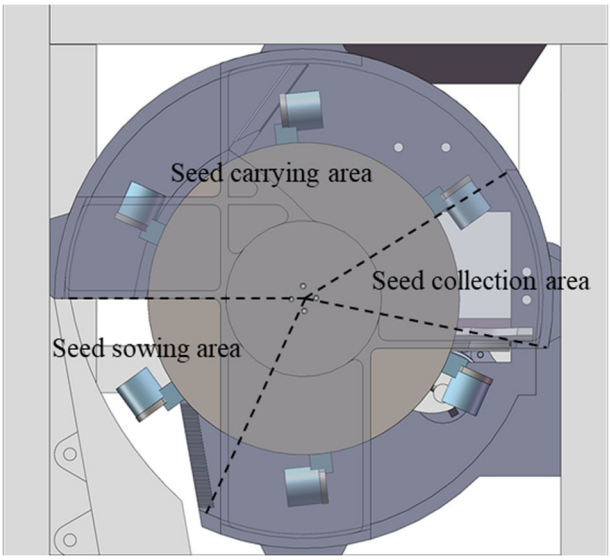


**Figure 2.** Schematic diagram of seeding disc partitioning.

*2.3. Design of Rotating Disc*

The most significant parameters of the rigid-flexible coupled garlic seeding device comprise the diameter of the rotating disc and the maximum number of seeding pockets that can be accommodated. The relationship between the number of seeding pockets and the diameter of the rotating disc, as well as the rotational speed, can be determined in order to ensure the density of garlic seeding, depending on the agronomic requirements of the process.

Obviously, the larger the diameter of the rotating disc, the greater the number of seeding pockets that can be accommodated. Consequently, the seeding disc rotation speed can be relatively lower, which is conducive to increasing the seeding disc seeding stability. In accordance with the rotating disc diameter $d_p$ and the rotational speed $n_p$, as well as the relationship between the forward speed of the planter $V_c$, the rotating disc diameter is determined to be 200 mm.

It has been demonstrated that the rotational speed of the rotating disc is directly proportional to the linear speed of the seeding pockets. An increase in the rotational speed results in a corresponding increase in the linear speed of the seeding pockets. This, in turn, has the effect of reducing the time available for the seed filling, which may lead to unstable capture of the seed. This paper sets the maximum linear velocity of the seeding pocket at 0.35 m/s, and according to Equation (1), the maximum rotational speed is 25.9 r/min.

$$\frac{d_p n_p \pi}{60} = 0.35 \text{ m/s} \tag{1}$$

where, $d_p$ is the diameter of rotating disc, m; $n_p$ is the rotational speed of rotating disc, r/min.

In order to ascertain the relationship between the spacing of the seeding pockets and the garlic plant spacing, it is necessary to establish the time required for the garlic seeding device to traverse the arc length between the two seeding pockets. This time must be equal to the time for the planter to pass through one garlic plant spacing, which gives

$$S_p = \frac{S_c d_p n_p \pi}{(1+\delta)60V_c} \tag{2}$$

where, $S_p$ is the arc length distance between seeding pockets, m; $V_c$ is the planter speed, m/s; $S_c$ is the garlic plant spacing, m; and $\delta$ is the ground wheel slip coefficient.

Garlic planting agronomic requirements stipulate that the plant spacing should be 80-120 mm, the planter forward speed is between 1-2 km/h, and the ground wheel slip coefficient is between 0.05-0.12. It is calculated from Equation (2) that the arc length between the seeding pockets is 35-112 mm.

According to Equation (3), the number of seeding pockets is to be determined as a range of 5 to 17. In this study, the value is set to be 6.

 doi:10.20944/preprints202509.0664.v1



$$n_s = \frac{d_p \pi}{S_p} \tag{3}$$

where, $n_s$ is the number of seeding pockets.

*2.4. Design of the Seeding Pocket*

The configuration of the seeding pocket exerts a significant influence on the seeding, and its design should be optimized in accordance with the dimensions of garlic seeds. A random selection of 300 "Jinxiang" garlic seeds was selected for the purpose of measuring the three-axis dimensions as a benchmark, as shown in Figure 3. It should be noted that the garlic seeds were procured via online retailers and have not been subject to any treatment prior to measurement in this section and the bench test in section 4. The cultivation of "Jinxiang" garlic is a pervasive practice in the Jiangsu region, particularly in the municipality of Jinxian. This variety is emblematic of the region's garlic production. The garlic seeds were divided into three levels, the results of which are shown in Table 1.


(a) length (b) width (c) thickness

**Figure 3** Dimensioning of three axes

**Table 1.** Three-axis dimensions of garlic seeds.

| Grade | Length/mm | Width/mm | Thickness/mm |
|---|---|---|---|
| 1 | 26.5~30.1 | 13.1~19.8 | 13.7~16.8 |
| 2 | 29.7~33.2 | 16~22.5 | 18.1~21.1 |
| 3 | 32.9~37 | 19.4~23.7 | 20.9~22.8 |

As illustrated in Figure 4, a volume-variable seeding pocket was designed, *H* and *R* are the depth and radius of the pocket, respectively. It can take 1 or 2 garlic seeds in the seed collection area, and then through the contraction of the metal sheet, it forces the excess garlic seeds with poor seed-occupying rate to fall off. Therefore, the radius of the metal sheet (*R*) and the depth of the seeding pocket (*H*) are very important.

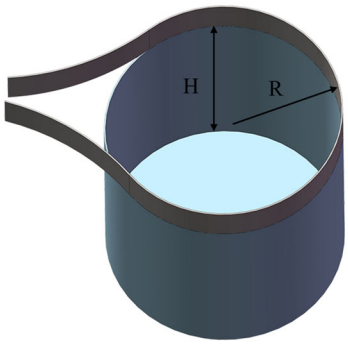


**Figure 4.** Seeding pocket.

 doi:10.20944/preprints202509.0664.v1



The radius of the metal sheet is selected according to the size distribution of garlic seeds. It is imperative that the diameter of the pocket is larger than the maximum width of the third-grade garlic seeds ($W_{3max}$) and smaller than the minimum length of the first-grade garlic seeds ($L_{1min}$). This is demonstrated in Equation 4. Consequently, the range of metal sheet diameter values was determined to be from 23.7 mm to 26.5 mm. In order to facilitate the subsequent analysis, these values were then rounded to 24 mm and 26 mm. And the radius of the metal sheets at the three levels of 12 mm, 12.5 mm and 13 mm is presented in this paper, respectively.

$$\begin{cases} 2R < L_{1min} \\ 2R > W_{3max} \end{cases} \tag{4}$$

The pocket's flexibility results in the garlic seed altering its posture upon entry. This can result in the seed adopting a horizontal lying posture, which can impede it falling off in the seed sowing area due to obstruction by the metal sheet. Therefore, it is necessary to determine the depth of the pocket. To facilitate the insertion of the garlic seeds into the pocket, the depth of the pocket ($H$), should be less than the minimum length of the first level of garlic seeds, denoted as $L_{1min}$. Furthermore, to ensure that the gravity center of the garlic seed remains within the pocket, it is essential that the depth of the pocket is bigger than the third level of the maximum length of the garlic seeds ($L_{3max}$). As shown in equation 5.

$$\begin{cases} H < L_{1min} \\ H > \dfrac{L_{3max}}{2} \end{cases} \tag{5}$$

According to the size data of garlic seeds, the pocket depth $H$ attains a median value of 22.25 mm within the interval [18.5, 26] and is thus rounded to 22 mm.

### *2.5. Design of the Retraction Control Mechanism*

The fixed disc, slide bar and slider constitute the mechanism that governs the opening and closing of the seeding pocket, and the configuration of the three components is illustrated in Figure 5.

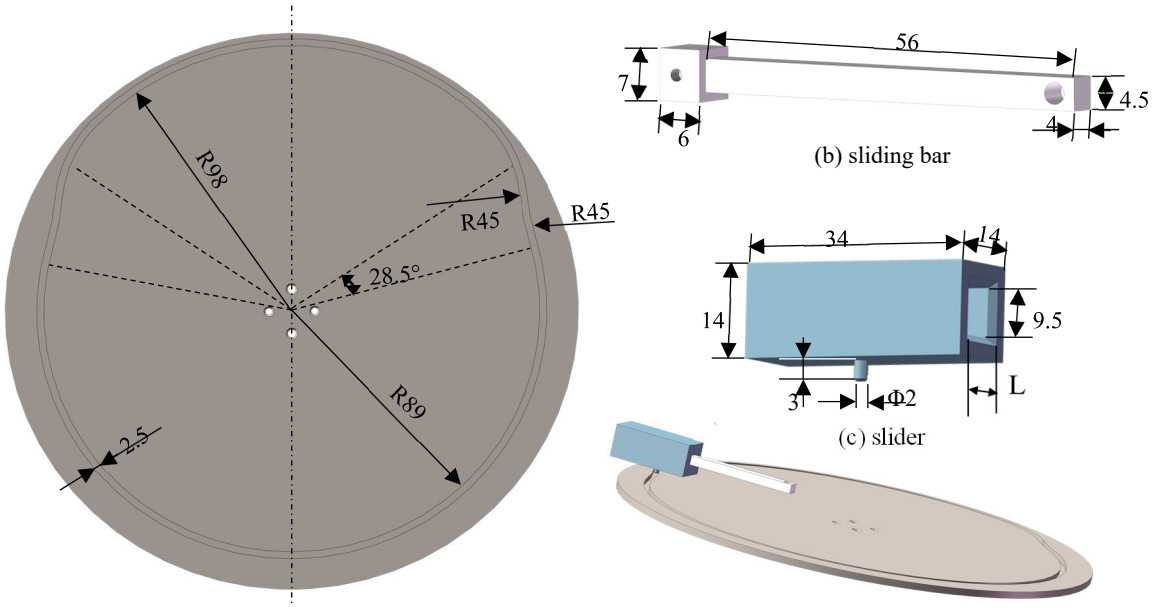


(a) fixed disc

(b) sliding bar

(c) slider

(d) assembly drawing

**Figure 5.** Retracting and Placing Control Mechanism (length unit: mm).

 doi:10.20944/preprints202509.0664.v1



The diameter of the fixed disc is equivalent to that of the rotating disc. The track on the fixed disc is pivotal in controlling the movement of the slider. The slider is equipped with an extended small cylindrical component, measuring 2 mm in diameter and 3 mm in length, which is to be inserted into the designed track. The width of the track is 2.5 mm, while its depth is 2.2 mm. This ensures that the slider can slide smoothly within the track.

The center of the seeding pocket is positioned at a distance of 21 mm from the end face of the slider bar. Upon entry of the slider into the track with a larger radius, the end face and inner wall of the slider result in the metal sheet being compressed, thereby causing the pocket to tighten. Concurrently, the end face of the slider exerts a force on the metal sheet, pushing it to the size of the maximal width of the tertiary garlic seeds, $W_{3max}$. It can thus be deduced that the radius of the large track on the fixed disc should be 21+12-23.7≈9 mm larger than the radius of the small track. Therefore, based on the size of the chamber, the radius of the larger track is set to 98 mm, and the radius of the smaller track is set to 89 mm. In order to facilitate the seamless transition of the slider through the arcs, two arcs with a radius of 45 mm are utilized to tangent to the large and small arcs, respectively. The angle of the transition zone is set at 28.5°.

As illustrated in Figure 5(c), the distance $L$ between the inner walls on the right side of the slider is a pivotal factor in determining the tightening force of the metal sheet, while the hole (5 mm × 5 mm) on the other side is for the passage of a rectangle (4.5 mm × 4 mm) sliding bar. In this study, the distances are determined in five levels according to the size of garlic seeds: 6 mm, 6.5 mm, 7 mm, 7.5 mm and 8 mm. A single-factor simulation analysis of the distance $L$ was conducted, with a rotational speed of 0.2 rad/s, a metal sheet thickness of 0.2 mm, and a pocket radius of 12.5 mm utilized. The outcomes of this analysis are presented in Table 2.

**Table 2.** Simulation results of single-factor test.

| Inner wall spacing/mm | 6 | 6.5 | 7 | 7.5 | 8 |
|---|---|---|---|---|---|
| Max stress of garlic seed/MPa | 4.94 | 3.66 | 3.47 | 2.86 | 1.48 |

As demonstrated in Table 2, the maximum stress experienced by garlic seeds increases with the reduction in $L$. Preliminary compression failure tests on garlic seed have indicated a critical stress of 3 MPa. It is therefore imperative to obtain a smaller closure size of metal sheet without damaging the garlic seeds. In this paper, the distance is taken to be 7.5 mm.

## 3. Simulation of the Seeding Process

### *3.1. Simulation Model Establishment*

The focus of this simulation (conducted in Abaqus 2020) is the entire process of seed picking, seed carrying and seed dropping by the seeding pocket through the opening and closing of the metal sheet. In this analysis, the existence of a flexible seeding pocket and a metal sheet result in the rest of the structure being designated as rigid bodies. It is imperative to consider the damage to the garlic seed during the tightening of the metal sheet, and for this reason, the garlic seed is set as an elastic body. The explicit dynamics analysis of finite element method was utilized to simulate the interaction between the metal sheet- pocket-garlic seed. The relevant material parameters are delineated in Table 3.

 doi:10.20944/preprints202509.0664.v1



**Table 3.** Material parameters.

| Material | Modulus of elasticity/MPa | Poisson's ratio | Density/t/mm$^3$ |
|---|---|---|---|
| Garlic seed | 23.82 | 0.25 [22] | $5.1\times10^{-9}$ |
| Metal sheet | 210000 | 0.3 | $7.8\times10^{-9}$ |
| Seeding Pocket [23] (cotton fabric) | 915 | 0.142 | $1.5\times10^{-9}$ |

In order to reduce the computational burden, the fixed disk with tracks retains only its track characteristics, as illustrated in Figure 6. The trajectory of the slider end as it moves along the track on the fixed disc is established by the one-dimensional rigid lines. Moreover, they function as a constituent that facilitates the actuation of the pocket's opening and closing mechanisms. Furthermore, the seeding pocket is modelled using two-dimensional membrane elements, incorporating a total of 1389 M3D4R elements and 6 M3D3 elements. The garlic seeds are modelled with three-dimensional solid elements, consisting of 189 C3D8R elements and 269 C3D4 elements. The metal sheet is modelled using beam elements, with a total of 112 B31 elements.

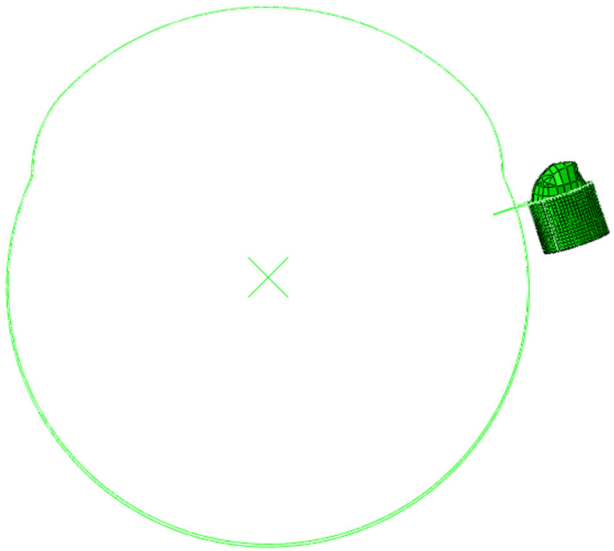

**Figure 6.** Finite element model.

Based on the actual boundary conditions, general contact is employed into the contact between garlic seed and seed box, garlic seed and pocket, garlic seed and metal sheet, track and slider. The normal behavior is set to hard contact, and the friction coefficient for the tangential behavior is set to 0.17. The metal sheet rotates around the center of the track, thereby restricting the remaining five degrees of freedom. Furthermore, a rotational speed around the x-axis is applied. The metal sheet and the pocket are bound together by tie constraints. In order to reduce the amount of calculation required, the trajectory of the contact point between the slider and the metal sheet is extracted. The trajectory of the slider is treated as a rigid body, which directly contacts the metal sheet, thereby controlling the opening and closing of the pocket. Furthermore, the garlic seeds are subjected to a gravitational acceleration of 9800 mm/s$^2$ pointing in the negative direction of the z-axis.

In the context of the simulations, the dynamic explicit step is utilized, and a mass scaling is implemented, which has resulted in a reduction in computation time. It is imperative to implement a step with ramp load in order to mitigate the consequences of mass scaling, which has the potential to induce excessive inertia. Over a period of one second, the system gradually accelerates from 0 to three levels: 0.15 rad/s, 0.2 rad/s, and 0.25 rad/s, respectively. In the subsequent step, the system undergoes rotation at a constant speed of 0.15 rad/s, 0.2 rad/s, and 0.25 rad/s, respectively.

 doi:10.20944/preprints202509.0664.v1



Preliminary simulation tests have demonstrated that the mass scaling setting of $10^{-6}$ s does not have a significant impact on the results.

### *3.2. Simulation Process of the Seeding*

In the seed-collecting process, the track radius gradually increases, the slider moves outward, and the metal sheet tightens the pocket, as seen in Figure 7(a). Meanwhile, the stress curve fluctuates and gradually rises with the step time. In the seed-carrying process, the garlic seeds are firmly fixed, and the internal stress oscillate slightly, as seen in Figure 7(b). And in the seed-sowing process, the track radius gradually decreases, the slider retreats, and the metal sheet recovers under the elastic action to open the pocket, which causes the internal stress of the garlic seed to gradually decrease, as seen in Figure 7(c). Finally, the garlic seed is separated from the pocket due to its gravity and centrifugal force, completing the seeding process. The stress experienced at the critical point of the garlic seed during the seeding process can be seen in Figure 7(d).

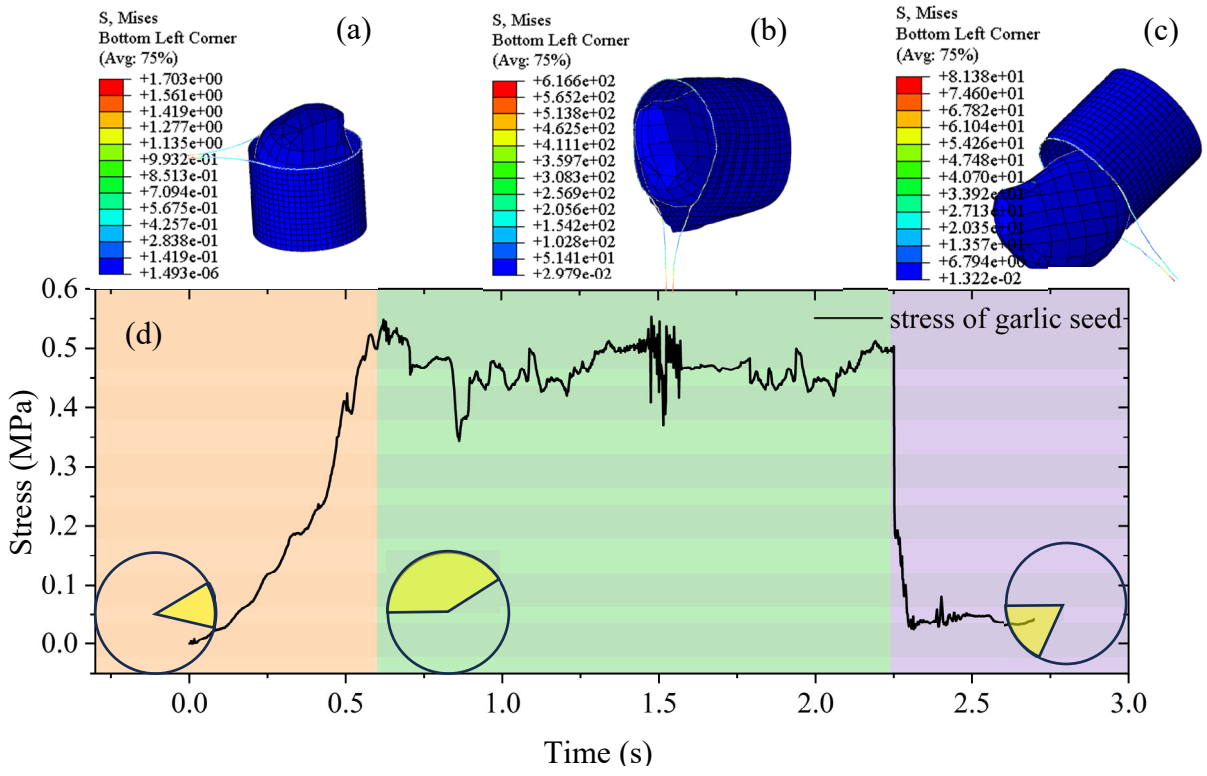


**Figure 7.** Seed stress in the seeding process ((a) Stress distribution in the seed collection area, (b) Stress distribution in the seed carrying area, (c) Stress distribution in the seed sowing area, (d) Stress-Time curve at the critical point of the garlic seed).

### *3.3. Multifactorial Analysis of Damage to Garlic Seed*

In order to investigate the damage of garlic seeds during the seeding process, the radius of the pocket ($x_1$), the rotational speed of the seeding disc ($x_2$) and the thickness of the metal sheet ($x_3$) were selected as the experimental variables according to the designed structure, the maximum stress on garlic seed during the seeding process was used as an evaluation index $Y_1$. The experimental factors and codes are shown in Table 4. $X_1$, $X_2$, and $X_3$ are coded values for the test factors. the test program and the results are shown in Table 5.

 doi:10.20944/preprints202509.0664.v1



**Table 4.** Test factors and codes.

| Code | Factors | | |
|---|---|---|---|
| | Pocket radius $x_1$/mm | Rotational speeds of seeding disc $x_2$/rad/s | Thickness of metal sheet $x_3$/mm |
| -1 | 12 | 0.15 | 0.15 |
| 0 | 12.5 | 0.2 | 0.2 |
| 1 | 13 | 0.25 | 0.25 |

**Table 5.** Test protocol and results for garlic seeds.

| No. | Factors | | | $Y_1$/MPa |
|---|---|---|---|---|
| | $X_1$ | $X_2$ | $X_3$ | |
| 1 | -1 | -1 | 0 | 1.99 |
| 2 | 1 | -1 | 0 | 1.31 |
| 3 | -1 | 1 | 0 | 0.77 |
| 4 | 1 | 1 | 0 | 0.91 |
| 5 | -1 | 0 | -1 | 0.603 |
| 6 | 1 | 0 | -1 | 0.428 |
| 7 | -1 | 0 | 1 | 0.84 |
| 8 | 1 | 0 | 1 | 0.684 |
| 9 | 0 | -1 | -1 | 2.03 |
| 10 | 0 | 1 | -1 | 1.31 |
| 11 | 0 | -1 | 1 | 2.03 |
| 12 | 0 | 1 | 1 | 2.17 |
| 13 | 0 | 0 | 0 | 2.55 |
| 14 | 0 | 0 | 0 | 2.86 |
| 15 | 0 | 0 | 0 | 2.73 |
| 16 | 0 | 0 | 0 | 2.57 |
| 17 | 0 | 0 | 0 | 2.37 |

As illustrated in Figure 8, the Mises equivalent stress (S) distribution of garlic seeds under pocket closing conditions was investigated in the 17 simulations. The action of the metal sheet is the primary source of stress on the garlic seed. Consequently, the garlic seed experiences the greatest level of stress in contact with the metal sheet, as illustrated in the red section of the figure. Preliminary compression failure tests on garlic seeds indicate that its critical stress for damage is approximately 3 MPa. While the maximum stress received by the garlic seeds in all 17 analyses was found not to exceed 3 MPa, indicating that the rigid-flexible coupling of garlic seed tray can significantly reduce the damage of garlic.

 doi:10.20944/preprints202509.0664.v1



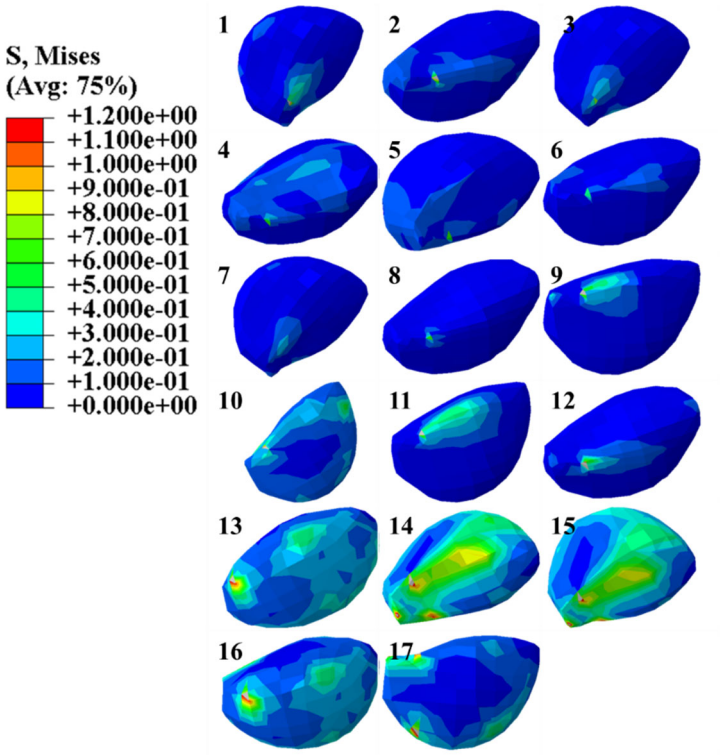


**Figure 8.** Mises equivalent stress (S) contour plot of garlic seeds.

The utilization of Design-Expert 13 software to conduct an analysis of variance on the garlic stress data presented in Table 5 yielded the results displayed in Table 6. The *P*-value of the maximum stress regression model is less than 0.01, which is deemed to be highly significant. In contrast, the *P*-value of the lack of fit is greater than 0.05, thereby indicating that lack of fit is not significant. A thorough examination of the *P*-value indicates that within the maximum stress regression model, $x_2$, $x_1^2$ and $x_3^2$ exert a profoundly significant influence on the model. The relative importance of these three factors in determining the impact of maximum stress on garlic seeds is determined by the rotational speed of the disc, the thickness of the sheet, and the radius of the pocket. Multiple linear regression analysis was conducted on the experimental results, and the multiple regression equation for the maximum stress of garlic seeds was obtained:

$$Y_1 = 2.62 - 0.11x_1 - 0.28x_2 + 0.17x_3 + 0.21x_1x_2 + 0.22x_2x_3 - 1.31x_1^2 - 0.06x_2^2 - 0.67x_3^2 \quad (6)$$

The utilization of response surface analysis method facilitates the observation of the influence of each interaction term on the maximum stress of garlic seeds. The interaction between the two factors on the evaluation index is then analyzed respectively, with the remaining factors taken as middle values, as demonstrated in Figure 9.

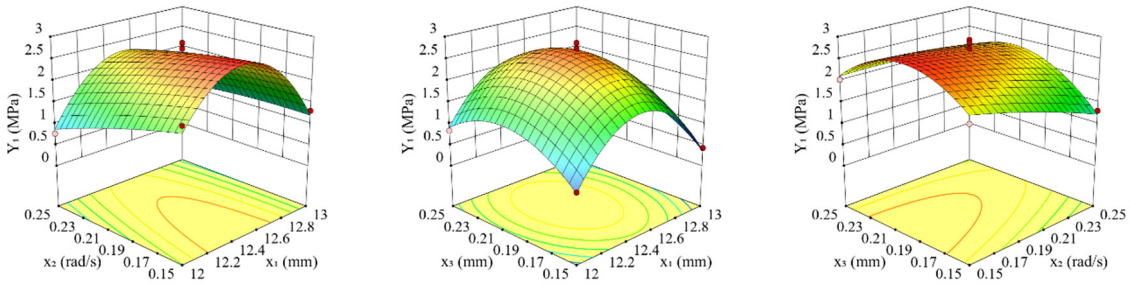


(a) $X_3 = 0$ (b) $X_2 = 0$ (c) $X_1 = 0$

 doi:10.20944/preprints202509.0664.v1



**Figure 9.** Response surface of the influence of various factors on the maximum stress of garlic seeds.

**Table 6.** Variance analysis of garlic stress.

| Source of variance | Garlic stress $Y_1$ | | | |
|---|---|---|---|---|
| | Sum of squares | Degree of freedom | $F$ | $P$ |
| Model | 10.91 | 9 | 28.58 | 0.0001 |
| $x_1$ | 0.0948 | 1 | 2.23 | 0.1786 |
| $x_2$ | 0.6050 | 1 | 14.26 | 0.0069 |
| $x_3$ | 0.2288 | 1 | 5.39 | 0.0532 |
| $x_1x_2$ | 0.1681 | 1 | 3.96 | 0.0868 |
| $x_1x_3$ | 0.0001 | 1 | 0.0021 | 0.9645 |
| $x_2x_3$ | 0.1849 | 1 | 4.36 | 0.0752 |
| $x_1^2$ | 7.21 | 1 | 169.94 | < 0.0001 |
| $x_2^2$ | 0.0164 | 1 | 0.3861 | 0.5541 |
| $x_3^2$ | 1.88 | 1 | 44.36 | 0.0003 |
| Residual | 0.2970 | 7 | | |
| Lack of Fit | 0.1575 | 3 | 1.51 | 0.3418 |
| Pure error | 0.1395 | 4 | | |
| Cor Total | 11.21 | 16 | | |

As illustrated in Figure 9(a), the interaction between the radius of the pocket and the rotational speed of the disc exerts a significant influence on the maximum stress of garlic seed during the seed picking process, under conditions where the thickness of the metal sheet is maintained at an intermediate level. When the rotational speed is maintained at a constant value, the maximum stress experienced by the garlic seed increases before decreasing in proportion to the increase in the radius of the pocket. Conversely, when the pocket radius is set at a specific value, the maximum stress experienced by the garlic seed gradually decreases in proportion to the increase in the rotational speed. As is apparent from the contour map, the image is of an elliptical nature. This finding indicates that the interaction between the pocket radius and the rotational speed is more obvious, and the effect of the pocket radius will be diminished as the rotational speed increases gradually.

As illustrated in Figure 9(b), the interaction between the pocket radius and the thickness of the metal sheet exerts a significant influence on the maximum stress, particularly when the rotational speed is maintained at the intermediate level. The maximum stress demonstrated a tendency to increase, followed by a subsequent decrease, in accordance with the augmentation of the pocket radius or the thickness of the metal sheet. As demonstrated by the contour plots, the images exhibited a high degree of circularity. This finding suggests that the interaction between the pocket radius and the metal sheet thickness is relatively balanced.

As illustrated in Figure 9(c), the interaction between the rotational speed and the thickness of the metal sheet exerts a significant influence on the maximum stress. This observation is made under the assumption that the pocket radius is maintained at the intermediate level. The maximum stress exhibited an increasing trend with an increase in the thickness of the metal sheet at a specific rotational speed, and a decreasing trend with an increase in the rotational speed at a constant thickness of the metal sheet. It was observed that the contour lines exhibited an elliptical shape, indicating that the interaction between the rotational speed and the thickness of the metal sheet was evident, and the impact of the thickness on the maximum stress was found to be diminished with an increase in the rotational speed.

 doi:10.20944/preprints202509.0664.v1



## 4. Bench Test

### *4.1. Test Preparation*

A test bench for the performance of the seeding device was constructed, as illustrated in Figure 10. The fixed disc, rotating disc, sliding bar and slider were manufactured using a 3D printer. Regarding the style of basketball bag, six pockets were created by wrapping six metal sheets with fabric. The driving motor of the rotating disc was selected as PFDE 7IK40CRGU-CF, with a rated power of 400 W. Furthermore, the model of the motor driving the seed disturbance plate was identified as WUP M425-402. According to GB/T 6973-2005, entitled "Testing methods of single seed drills (precision drills)" [24], the number of seeds recorded as the statistical object during the operation of the seeding device when it is functioning at a constant value was 251. Each experiment was replicated five times, and the mean value was calculated.

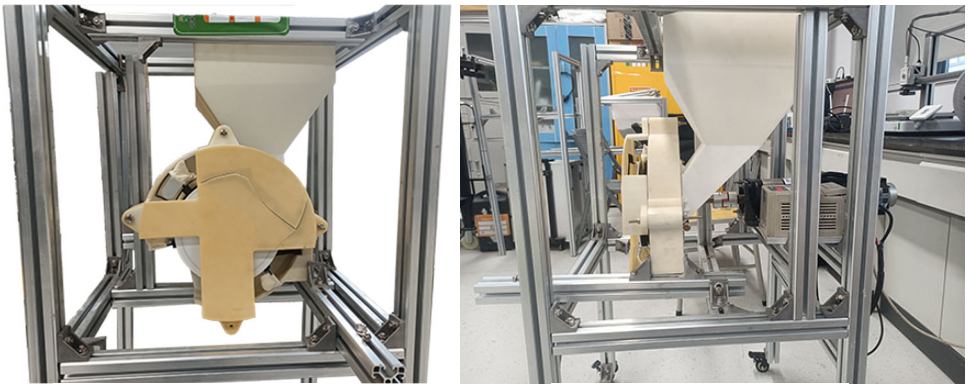

(a) Front view of test bench (b) Side view of test bench

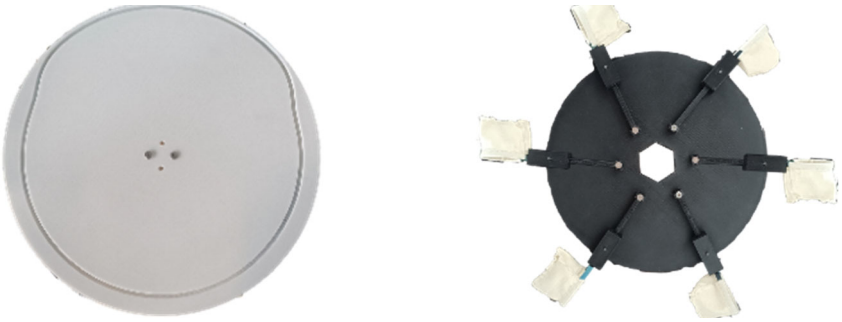

(c) Fixed disc (d) Rotating disc with seeding pockets

**Figure 10.** Seeding device bench test.

Around 400 garlic seeds were deposited into the designated seed box, after which the motor is activated. The rotation of the rotating disc is initiated, and the disturbance plate commences oscillation. The seeding pockets located on the rotating disc pass upwards through the seed box, capture a garlic seed, and commence tightening. The seed is then transported to the designated seed sowing area, where it undergoes a process of opening of the seeding pockets. The garlic seed then falls into the collection box under the action of gravity.

The present experiment is centered on the investigation of damage to garlic seeds, with the primary objective being the collection of data on garlic seed damage. Concurrently, the single-seed rate and leakage rate are also being recorded. The collection of data pertaining to damage rate $Y_2$, the single-seed rate $Y_3$, and the leakage rate $Y_4$ is conducted by means of manual calculation, followed by equations (1-3).

$$Y_2 = \frac{N_{damage}}{N_{total}} \times 100\% \quad (7)$$

 doi:10.20944/preprints202509.0664.v1



$$Y_3 = \frac{N_{single}}{N_{total}} \times 100\% \quad (8)$$

$$Y_4 = \frac{N_{leakage}}{N_{total}} \times 100\% \quad (9)$$

where, $N_{damage}$, $N_{single}$, $N_{leakage}$ and $N_{total}$ are the numbers of damage seed, single seed, leakage seed, and the total seed, respectively.

*4.2. Analysis of Test Results*

The multi-factor test was conducted, with the damage rate ($Y_2$), single-seed rate ($Y_3$) and the seed leakage rate ($Y_4$) as the evaluations and the factor coding values ($x_1$, $x_2$ and $x_3$). The test results are presented in Table 7. Given that the damage rate $Y_2$ is zero, it was determined that further analysis was not required.

**Table 7.** Bench test results.

| No. | Factors | | | Performance indexes | | |
|---|---|---|---|---|---|---|
| | $X_1$ | $X_2$ | $X_3$ | Damage rate $Y_2$/% | Single seed rate $Y_3$/% | Leakage rate $Y_4$/% |
| 1 | 0 | 0 | 0 | 0 | 74.8 | 13.6 |
| 2 | 1 | 0 | -1 | 0 | 72.9 | 14.6 |
| 3 | 0 | 0 | 0 | 0 | 73.9 | 14.1 |
| 4 | 1 | 1 | 0 | 0 | 68.6 | 16.9 |
| 5 | 1 | 0 | 1 | 0 | 72.8 | 14.7 |
| 6 | -1 | -1 | 0 | 0 | 70.0 | 16.1 |
| 7 | 0 | 0 | 0 | 0 | 75.5 | 13.2 |
| 8 | 0 | -1 | -1 | 0 | 73.0 | 15.3 |
| 9 | -1 | 0 | -1 | 0 | 79.1 | 11.4 |
| 10 | 1 | -1 | 0 | 0 | 68.8 | 16.8 |
| 11 | 0 | 1 | 1 | 0 | 75.0 | 13.5 |
| 12 | 0 | 0 | 0 | 0 | 76.5 | 12.8 |
| 13 | 0 | 1 | -1 | 0 | 72.5 | 14.8 |
| 14 | 0 | 0 | 0 | 0 | 77.2 | 12.4 |
| 15 | -1 | 0 | 1 | 0 | 76.2 | 15.1 |
| 16 | 0 | -1 | 1 | 0 | 66.9 | 17.8 |
| 17 | -1 | 1 | 0 | 0 | 71.9 | 12.9 |

ANOVA was performed on the damage rate, single-seed rate and leakage rate, as shown in Table 8, using Design-Expert 13 software. The P-values of the two regression models are less than 0.01, which is highly significant; however, the *P*-values of the lack of fit are greater than 0.05, indicating that the lack of fit is not significant. A thorough examination of the P-value reveals that, within the single seed rate regression model, both $x_1$ and $x_2^2$ exhibited a significant impact on the model, while $x_2x_3$ demonstrated a significant effect. The three factors affecting the single seed rate were the pocket radius, the rotational speed, and the thickness of the metal sheet, in that order of importance. In the leakage rate regression model, $x_1$, $x_2$, $x_2^2$ exhibited a highly significant effect on the model, while $x_3$, $x_1x_3$, $x_2x_3$ demonstrated a significant effect. The three factors affecting the seed leakage rate were the rotational speed, the pocket radius, and the thickness of the metal sheet, in order of importance. Multiple linear regression was fitted to the experimental results to obtain the multiple regression equations for single-seed rate $Y_3$ and seed leakage rate $Y_4$ (Equations (10)).

 doi:10.20944/preprints202509.0664.v1



**Table 8.** Variance analysis for bench tests.

| Source of variance | Single seed rate $Y_3$ | | | | Leakage rate $Y_4$ | | | |
|---|---|---|---|---|---|---|---|---|
| | Sum of squares | Degree of freedom | $F$ | $P$ | Sum of squares | Degree of freedom | $F$ | $P$ |
| Model | 161.33 | 9 | 8.91 | 0.0044 | 45.33 | 9 | 10.29 | 0.0028 |
| $X_1$ | 24.64 | 1 | 12.24 | 0.0100 | 7.03 | 1 | 14.37 | 0.0068 |
| $X_2$ | 11.03 | 1 | 5.48 | 0.0518 | 7.80 | 1 | 15.94 | 0.0052 |
| $X_3$ | 5.55 | 1 | 2.76 | 0.1406 | 3.12 | 1 | 6.39 | 0.0394 |
| $X_1X_2$ | 1.12 | 1 | 0.5589 | 0.4791 | 2.72 | 1 | 5.56 | 0.0504 |
| $X_1X_3$ | 2.00 | 1 | 0.9935 | 0.3521 | 3.24 | 1 | 6.62 | 0.0368 |
| $X_2X_3$ | 18.86 | 1 | 9.37 | 0.0183 | 3.61 | 1 | 7.38 | 0.0299 |
| $X_1^2$ | 6.01 | 1 | 2.98 | 0.1277 | 1.17 | 1 | 2.39 | 0.1657 |
| $X_2^2$ | 88.24 | 1 | 43.85 | 0.0003 | 15.64 | 1 | 31.97 | 0.0008 |
| $X_3^2$ | 3.05 | 1 | 1.51 | 0.2581 | 0.1727 | 1 | 0.3528 | 0.5712 |
| Residual | 14.09 | 7 | | | 3.43 | 7 | | |
| Lack of Fit | 7.55 | 3 | 1.54 | 0.3349 | 1.66 | 3 | 1.25 | 0.4028 |
| Pure error | 6.54 | 4 | | | 1.77 | 4 | | |
| Cor Total | 175.42 | 16 | | | 48.76 | 16 | | |

$$\begin{cases} Y_3 = 75.6 - 1.8x_1 + 1.2x_2 - 0.8x_3 - 0.5x_1x_2 + 0.7 \\ \quad x_1x_3 + 2.2x_2x_3 - 1.2x_1^2 - 4.6x_2^2 + 0.9x_3^2 \\ Y_4 = 13.2 + 0.9x_1 - 1.0x_2 + 0.6x_3 + 0.8x_1x_2 - 0.9 \\ \quad x_1x_3 - 1.0x_2x_3 + 0.5x_1^2 + 1.9x_2^2 + 0.2x_3^2 \end{cases} \tag{10}$$

As illustrated in Figure 11, the response surface for the single seed rate $Y_3$ is depicted. And in Figure 11(a), the interaction between the pocket radius and the rotational speed of the seed-picking disc exerts a significant influence on the single seed rate, with the thickness of the metal sheet fixed at an intermediate level. When the rotational speed is constant, the single seed rate decreases as the pocket radius increases. When the pocket radius is held at a constant value, the single seed rate initially increases and subsequently decreases as the rotational speed rises.

As illustrated in Figure 11(b), the interaction between the pocket radius and the thickness of the metal sheet exerts a significant influence on the single seed rate when the rotational speed is set to an intermediate level. When the metal sheet thickness is fixed, the single seed rate decreases as the pocket radius increases. Conversely, when the pocket radius is fixed, the single seed rate decreases as the metal sheet thickness increases. It is evident that as the radius increases, the effect of the metal sheet thickness gradually diminishes.

As illustrated in Figure 11(c), the interaction between the rotation speed and the thickness of the metal sheet exerts a significant influence on the single seed rate, under the condition that the radius of the pocket is designated as the midpoint. It has been observed that as the rotational speed decreases, the single seed rate concomitantly decreases with an increase in the thickness of the metal sheet. Conversely, at elevated rotational speeds, the single seed rate increases in proportion to the thickness of the metal sheet. When the thickness of the metal sheet was constant, the single seed rate increased initially and then decreased with an increase in the rotational speed.

 doi:10.20944/preprints202509.0664.v1



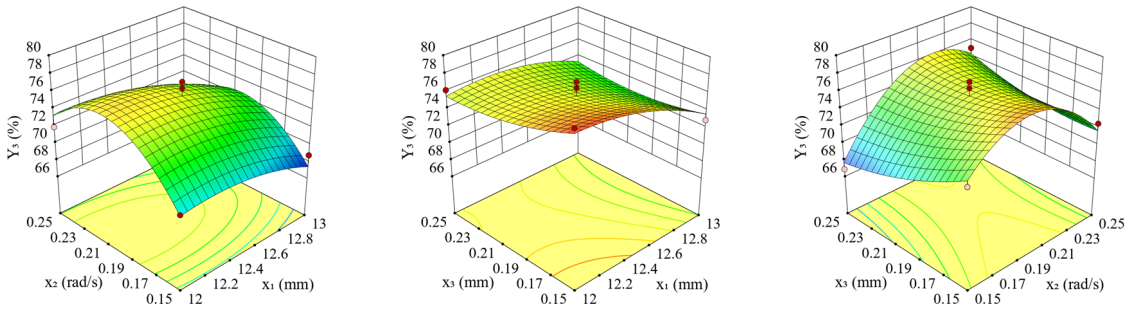


(a) $X_3 = 0$ (b) $X_2 = 0$ (c) $X_1 = 0$

**Figure 11.** Response surface of the effect of various factors on the single seed rate.

As shown in Figure 12, the response surface for the seed leakage rate $Y_4$ is presented. And in Figure 12(a), the interaction between the pocket radius and the rotational speed of the seed-picking disc exerts a significant influence on the seed leakage rate, with the thickness of the metal sheet fixed at an intermediate level. The initial decrease in the seed leakage rate is followed by an increase as the pocket radius is increased when the rotational speed is maintained at a low level. Conversely, the seed leakage rate exhibits an increase as the pocket radius is increased when the rotational speed is elevated. It has been demonstrated that the seed leakage rate is subject to a decrease in accordance with an increase in the rotational speed, when the pocket radius is low. Conversely, an increase in the rotational speed has been observed to result in a decrease in the seed leakage rate, followed by an increase, when the pocket radius is high.

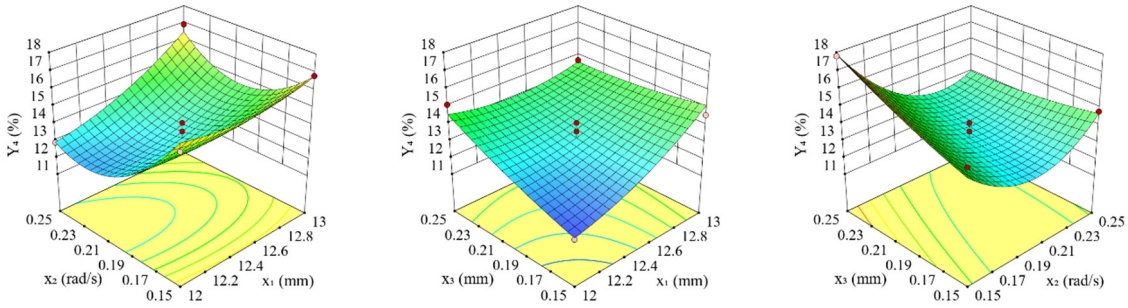


(a) $X_3 = 0$ (b) $X_2 = 0$ (c) $X_1 = 0$

**Figure 12.** Response surface of the effect of factors on the seed leakage rate.

As illustrated in Figure 12(b), the interaction between pocket radius and metal sheet thickness exerts a significant influence on the rate of seed leakage, under conditions wherein the rotational speed is maintained at an intermediate level. When the thickness of the metal sheet is taken at a high level, the seed leakage rate decreases and then increases with the increase of the pocket radius; conversely, when the thickness of the metal sheet is taken at a low level, the seed leakage rate increases with the increase of the pocket radius. When the pocket radius is taken at a high level, the seed leakage rate decreases with the increase of the thickness of the metal sheet; conversely, when the pocket radius is taken at a low level, the seed leakage rate increases with the increase of the thickness of the metal sheet.

It can be seen in Figure 12(c), the interaction between the rotational speed and the thickness of the metal sheet has a significant impact on the seed leakage rate, when the pocket radius is maintained at an intermediate level. As the thickness of the metal sheet increases, the leakage rate rises concomitantly with the low rotational speed. Conversely, as the thickness of the metal sheet increases, the leakage rate decreases with a high rotational speed. When the thickness of the metal

 doi:10.20944/preprints202509.0664.v1



sheet is constant, the seed leakage rate experiences a decrease, followed by an increase, with the rise in the rotational speed.

A comparison of Figures 11 and 12 reveals that the influence of each factor on the single-seed rate and seed leakage rate is relatively similar. In fact, these two sets of data are inherently related: an increase in the single-seed rate inevitably leads to a decrease in the seed leakage rate. This confirms the reliability of our analysis process.

The following conditions (Equation (11)) were employed to ascertain the level combinations that would result in the single-seed rate attaining its maximum value, the seed leakage rate attaining its minimum value, and the maximum stress of garlic seed falling below the limit value, utilizing the optimization function of the software.

$$\begin{cases} 0 < Y_1 < 3 \\ max\ Y_3 \\ min\ Y_4 \\ s.t. \begin{cases} -1 \le X_1 \le 1 \\ -1 \le X_2 \le 1 \\ -1 \le X_3 \le 1 \end{cases} \end{cases} \tag{11}$$

Following a thorough analysis of the optimal working parameters, the following conclusions were reached: the radius of the pocket was established at 12 mm, the rotational speed of the seed-picking disc was set at 0.21 rad/s, and the thickness of the metal sheet was determined to be 0.15 mm. In the context of this specific combination, the model predicts that the single-seed rate is 78.4%, the seed leakage rate is 11.4%, and the maximum stress experienced by the garlic seed is 0.535 MPa.

Bench tests using the optimal combination of parameters revealed that zero damage to the garlic seed was achieved despite the lower single grain rate. Compared with spoon-chain and finger-clamp types, this device's sowing quality is not ideal. However, simulations and experiments have proven that the device can sow garlic seeds without causing any damage. Further optimization could target the single-seed rate and leakage rate to improve sowing quality.

## 5. Conclusions

The problem of a high damage rate of garlic seeds by traditional seeding device has been identified as a priority for investigation. This study has therefore designed a new type of garlic seeding device with rigid-flexible coupling, and determined its key structural parameters through theoretical analysis, simulation calculation and experimental test. The primary conclusions that can be drawn from this analysis are as follows:

(1) Orthogonal simulation tests have been conducted to assess the impact of different conditions on the stress of garlic seeds. The results indicate that under conditions of 7.5 mm inner wall spacing, the stress levels of all 17 garlic seeds remained below 3 MPa, demonstrating that this design significantly reduces garlic damage.

(2) The Box-Behnken experimental design method was employed to conduct a three-factor, three-level regression orthogonal test. The findings revealed that the seeding effect attained its optimal level when the parameters were set to a pocket radius of 12 mm, a rotational speed of 0.21 rad/s, and a thickness of 0.15 mm for the metal sheet. This resulted in a 78.4% single-seed rate, accompanied by a leakage rate of 11.4%. The maximum stress experienced by the garlic seed was recorded as 0.535 MPa.

**Author Contributions:** Conceptualization, Y. Wang and H. Li.; methodology, S. Wang; software, S. Wang; validation, S. Wang, Y. Meng and X. Zhang; formal analysis, S. Wang and Y. Meng; investigation, S. Wang; resources, Y. Wang and H. Li.; data curation, S. Wang and Y. Meng; writing—original draft preparation, S. Wang; writing—review and editing, Y. Meng and Y. Wang; visualization, S. Wang and Y. Meng; supervision, H. Li.; project administration, Y. Wang and H. Li.; funding acquisition, Y. Wang and H. Li. All authors have read and agreed to the published version of the manuscript.

**Data Availability Statement:** "The data presented in this study were collected during the year 2025 and are available on request from the corresponding author."

**Acknowledgments:** This work was supported by the Jiangsu Province Demonstration and Promotion of Modern Agricultural Equipment and Technology (No. NJ2021-12, NJ2022-09), Integrated Research, Development, Manufacturing, Promotion and Application Pilot Program for Agricultural Machinery (No. JSYTH11) and Nanjing Modern Agricultural Machinery and Equipment and Technological Innovation Demonstration Project (No. NJ[2023]07)

**Conflicts of Interest:** "The authors declare no conflicts of interest."

## References

1. Cui, Z.C.; Liu, X.C; Chen, Y.S. Status, problems and countermeasures of whole mechanized production of garlic in China. *Journal of Chinese Agricultural Mechanization*, **2023**, 44, 239-243. https://doi.org/10.13733/j.jcam.issn.2095-5553.2023.06.034
2. Zhu, H.M; Evaluation and analysis on China's garlic export trade and international competitiveness. *China Cucurbits and Vegetables*, **2022**, 35, 111-116. https://doi.org/10.3969/j.issn.1673-2871.2022.10.019
3. Li, S.P.; Lu, S.; Cui, A.L. Treatment Effect of Garlic Extract on Escherichia coli-induced Rabbit Endometritis. *Progress in Veterinary Medicine*, **2025**, 46, 52-57. https://doi.org/10.16437/j.cnki.1007-5038.2025.07.014
4. Meng, L.Y; Zhang, J.L; Song, X.T. Study on the function of lowering blood lipid of garlic oil. *Chinese Journal of Public Health Engineering*, **2016**, 15, 247-249. https://doi.org/10.19937/j.issn.1671-4199.2016.03.018
5. Pu, C; Hu, H.B; Kuang, H.X. Research progress on antiviral effects of Allium sativum and its active ingredients. *Chinese Traditional and Herbal Drugs*, **2022**, 53, 2174-2183. https://doi.org/10.7501/j.issn.0253-2670.2022.07.028
6. Gao, L.X.; Li, X.F.; Jie; X. Investigation on Characteristics and Ratio of Soybean Kernel Mechanical Damage. *Journal of Shenyang Agricultural University*, **2010**, 41, 55-58. https://doi.org/10.3969/j.issn.1000-1700.2010.01.012
7. Li, J.Y; Su, N.N.; Hu, J.L. Numerical analysis and experiment of abrasive flow machining microhole structure based on CFD-DEM coupling. *Transactions of the Chinese Society of Agricultural Engineering*, **2018**, 34, 80-88. https://doi.org/10.11975/j.issn.1002-6819.2018.16.011
8. Gao, X.J.; Cui, T.; Zhou, Z.Y. DEM study of particle motion in novel high-speed seed metering device. *Advanced Powder Technology*, **2021**, 32, 1438-1449. https://doi.org/10.1016/j.apt.2021.03.002
9. Li, C.; Cui, T.; Zhang, D.X. Design and experiment of a centrifugal filling and cleaning high-speed precision seed metering device for maize. *Journal of Cleaner Production*, **2023**, 426, 139083. https://doi.org/10.1016/j.jclepro.2023.139083
10. Landahl, S.; Terry, L.A. Detection of internal defects in onion bulbs by means of single-point and scanning laser Doppler vibrometry. *Biosystems Engineering*, **2022**, 221, 258-273. https://doi.org/10.1016/j.biosystemseng.2022.07.004
11. Wang, S.S.; Zeng, Q.T.; Ni, W.J. ODP-Transformer: Interpretation of pest classification results using image caption generation techniques. *Computers and Electronics in Agriculture*, **2023,** 209, 107863. https://doi.org/10.1016/j.compag.2023.107863
12. Ding, Y.; Li, H.; Gao, J.; Yu, H.; Wang, Y.; Feng, D. Parameter Optimization of Finger Clip Plate Garlic Seed-Metering Device. *Agriculture*, **2023**, 13, 2071. https://doi.org/10.3390/agriculture13112071
13. Li, T.H.; Huang, S.H.; Niu, Z.R. Optimization and experiment of planting perpendicularity of planetary wheel garlic planter. *Transactions of the Chinese Society of Agricultural Engineering*, **2020**, 36, 37-45. https://doi.org/10.11975/j.issn.1002-6819.2020.03.005
14. Hou, J.L.; Wang, H.X.; Niu, Z.R. Discrete element simulation and experiment of picking and clearing performance of garlic seed-picking device. *Transactions of the Chinese Society of Agricultural Engineering*, **2019,** 35, 48-57. https://doi.org/10.11975/j.issn.1002-6819.2019.24.006
15. Hou, J.L.; Liu, Q.C.; Li, T.H. Design and experiment of the garlic seed metering device with double seed-filling chambers. *Transactions of the Chinese Society of Agricultural Engineering*, **2021**, 37, 21-32. https://doi.org/10.11975/j.issn.1002-6819.2021.14.003
16. Geng, A.J.; Li, X.Y.; Hou, J.L. Design and experiment of automatic directing garlic planter. *Transactions of the Chinese Society of Agricultural Engineering*, **2018**, 34, 17-25. https://doi.org/10.11975/j.issn.1002-6819.2018.11.003

 doi:10.20944/preprints202509.0664.v1



17. Zilpilwar, S; Yadav, R.; Jakasania, R. Development and Performance Evaluation of Metering Mechanism for Planting Garlic Cloves. *Agricultural research (India : Online)*, **2021**, 10, 274-284.https://doi.org/10.1007/s40003-020-00492-1
18. Ling, L.; Wu, G.W.; Wen, C.K. Influence of speed measurement method on performance of an electric-drive maize precision planter. *Biosystems Engineering*, **2024**, 238, 175-187.https://doi.org/10.1016/j.biosystemseng.2024.01.014
19. Zhang, C.L.; Zhang, X.Y.; Zheng, Z.H. Numerical Simulation and Test of the Disturbance Air Suction Garlic Seed Metering Device. *Machines*, 2022, 10, 11-27. https://doi.org/10.3390/machines10121127
20. Ding, L.; Yang, L.; Zhang, D.X. Effect of seed adsorption posture of corn air-suction metering device on seed feeding performance. Transactions of the Chinese Society for Agricultural Machinery, 2021, 52, 40-50. https://doi.org/10.6041/j.issn.1000-1298.2021.07.004
21. Zhang, Q.; Wang, Y.J.; Li, H.; Gao, J.F.; Ding, Y.G. Optimization of A Precision Symmetric Finger Clamping Garlic Seed-Metering Device. *Frontiers of Agricultural Science & Engineering*, **2024**, 11(4): 626–641. https://doi.org/10.15302/J-FASE-2024555
22. Li, H.; Meng, Y.B.; Qi, X.D. Discrete Element Modelling Method and Parameter Calibration of Garlic Species Based on Bonding V2 Model. *Transactions of the Chinese Society for Agricultural Machinery*, **2025**, 56,150-157+159. https://doi.org/10.6041/j.issn.1000-1298.2025.07.013
23. Hu, M.J.; Zhou, Y.; Tang, Z.C. Mechanical properties of the delinted and coated cottonseed. *Journal of Anhui Agricultural University*, **2018**, 45, 175-180. https://doi.org/ 10.13610/j.cnki.1672-352x.20180302.010
24. GB_T6973-2005; Testing methods of single seed drills (precision drills). China Standards Press: Beijing, Chian, 2005.